C.P. No. 1298

C.P. No. 1298

PROCUREMENT EXECUTIVE, MINISTRY OF DEFENCE

AERONAUTICAL RESEARCH COUNCIL

CURRENT PAPERS

Flight Determination of the Rudder Power and Directional Stability of the Fairey Delta 2 Aircraft Using a Wingtip Parachute

by

G. Ingle

Aerodynamics Dept., R.A.E., Bedford

LONDON: HER MAJESTY'S STATIONERY OFFICE

1974

PRICE 65*p* NET

UDC 533.694.542 : 533.6.013.415 : 533.666.2

CP No.1298 *
February 1973

FLIGHT DETERMINATION OF THE RUDDER POWER AND DIRECTIONAL STABILITY OF THE FAIREY DELTA 2 AIRCRAFT USING A WINGTIP PARACHUTE

by

G. Ingle

SUMMARY

The wingtip parachute technique has been used to extract the rudder power derivative, n_ζ, for the Fairey Delta 2 research aircraft. The flight tests have revealed that n_ζ has a considerably smaller value than tunnel tests suggested, and it is believed that this is due to the aeroelasticity of the fin and rudder, and possibly to unrepresentative flow over the rear of the wind-tunnel model.

Once n_ζ was obtained, the directional stability derivative, n_v, was derived on the assumption that the derivative n_ξ was small. The values of the derivative n_v obtained by this technique agree well with those from other flight tests and reasonably well with tunnel test results.

---

* Replaces RAE Technical Report 73025 - ARC 34852

CONTENTS

1 INTRODUCTION

The wingtip-deployed parachute offers a means of extracting two important aircraft lateral stability derivatives, namely the rudder yawing power n_ζ, and the directional stability derivative, n_v. A parachute deployed from near a wingtip can be used to exert a known yawing moment on the aircraft. The derivative n_ζ may be derived once the increment in rudder angle between the sideslip trim curves for the basic aircraft and for the parachute streamed case is determined. An approximation to the derivative n_v can then be determined from the trim curves and n_ζ.

In principle, static derivatives associated with all six degrees of freedom may be obtained by this technique since, in general, the parachute exerts a force or moment along or about all three stability axes of the aircraft. But in practice the degrees of freedom principally involved are those expressing the longitudinal forces and the yawing moment; any induced normal and side-loads and pitching moment are small, and the rolling moment only becomes significant at high incidence. These small effects are liable to be masked by scatter and the measurement accuracy would be very low.

This paper describes the extraction of n_ζ and n_v for the Fairey Delta 2 research aircraft following flight tests at RAE Bedford in 1966. Flight trials of the parachute installation had previously been conducted on a Venom aircraft[1] and had proved the feasibility of the method.

The measured values of n_ζ and n_v are compared with those obtained from wind tunnel tests[2,3], and n_v is compared with the re-analysed results from time vector analysis of dutch rolls reported previously[4].

2 DESCRIPTION OF AIRCRAFT

The Fairey Delta 2 (FD2), Figs.1 and 2, is a research aircraft built to investigate the aerodynamic characteristics of a 60° delta wing configuration at subsonic, transonic and supersonic speeds. The wing, of 4% thickness/chord ratio, has no twist, camber or dihedral and the trailing-edge is unswept. The elevators occupy the inboard half of the wing trailing-edge and the ailerons the remainder outboard to the tip. The ailerons move differentially about a rigging angle approximately 3° up from the wing chordal plane. The full span rudder is hinged to the highly swept fin. A duplicated hydraulic system is used to operate the flying controls *via* irreversible jacks and artificial feel is provided by springs. Leading dimensions are given in Table 1.

The power plant is a Rolls Royce Avon RA28R turbojet with non-variable reheat. The two-position eyelid type nozzle is open with reheat selected. For improved pilot visibility at low speeds the nose assembly, including the cockpit, may be drooped 10^{o} relative to the main fuselage.

3 DESCRIPTION OF TEST EQUIPMENT

3.1 The wingtip parachute installation

3.1.1 The Venom installation trials

Prior to installation on the Fairey Delta 2, the wingtip parachute was tested on a Venom aircraft[1]. Open-jet blower trials verified the streaming operation of the parachute on the Venom wing. This installation was found to be reliable in flight and the streaming and jettison operations functioned satisfactorily. However, the parachute did exhibit a coning phenomenon where the strop described a conical motion at some 1½ to 3 Hz with a maximum included angle of about 20^{o}. This leads to variations in the load exerted by the parachute in phase with the coning. A similar motion was found to occur with the FD2 installation.

3.1.2 The FD2 installation

The FD2 parachute installation (Fig.3) was virtually identical to that on the Venom except that it was fitted to the port instead of the starboard wingtip. The parachute strop was connected to the top of a post, 0.37m tall, through which the loads were transmitted *via* a support structure into the wing.

Before deployment, the parachute was stowed in a pack on a platform at the base of the post, the pack being held fast by cords. A fairing was fitted round the post to shield it from aerodynamic loads.

The parachute strop was attached to the post by means of a universal joint consisting of a swivelling cap and a yoke which permitted lateral and vertical strop movement. An explosive bolt, fitted between the strop and yoke could be fired electrically by the pilot to jettison the parachute. This bolt would be fired automatically in the event of the pack assembly coming adrift before the parachute had been streamed. A swivel joint at the bolt end permitted parachute rotation without the rigging lines becoming twisted. Fig.3 shows the installation and Ref.1 gives a more detailed description of the assembly.

The parachutes were of two sizes, 0.46m and 0.76m diameter, and the latter was designed to produce 4450N drag at Mach 1 at 40000ft (12200m) altitude. This

maximum permissible load was dictated by aircraft structural and aerodynamic limitations. The parachutes were of the 'shaped-gore' type and the fabric porosity was 10 m/s for the standard pressure difference of 3.86 N/m^2 of water across the fabric.

3.1.3 Operating limitations

The FD2 trials were not completely trouble free, principally because the stowed parachute arrangement was not altogether satisfactory, and on one occasion the parachute did not deploy on the selection of 'stream'. Inadvertent streaming also occurred and it was found that at around 300 kn ias the pack was liable to come adrift, providing a limit to the climbing speed. These problems were not encountered on the Venom trials, presumably because of the different flow fields existing at the wingtips of the two aircraft. The method of retaining the pack was slightly modified to ensure that the parachute would deploy when required.

3.2 Instrumentation associated with the installation

The parachute post was fitted with strain gauges near the base on all four faces. There were two four-active-arm strain gauge bridges and the gauges from each bridge were bonded in pairs on opposite faces of the post. The rearwards and lateral loads on the post were therefore sensed. The bridge outputs were recorded and the supply voltage across the bridges was also monitored.

A potentiometer was used to monitor the strop angle relative to the post axis.

The post was calibrated off the aircraft and the strain gauge outputs were found to be adequately linear with acceptable hysteresis characteristics. Cross-loading effects (the change in output from one bridge due to loading of the other) were also deemed small. To reduce any problems due to strain gauge drift, the outputs just before parachute stream were taken as referring to zero load. The calibrations were corrected for any change in bridge supply voltage.

The other instrumentation relevant to the tests included

Parameter	range available
Sideslip angle	$\pm 5^o$
Incidence	0 to $+10^o$ and -8^o to $+25^o$
Rudder angle	$\pm 9^o$
Aileron angle	$\pm 4^o$ and $\pm 17^o$
Free stream dynamic pressure	0 to 91000 N/m^2
Ambient static pressure	102 000 to 11000N/m^2 absolute
Free stream total temperature	220^o to 375^oK
Rate of roll	$\pm 20^o/s$
Rate of yaw	$\pm 4^o/s$

Sideslip and incidence were obtained from wind vanes mounted on the pitot/static boom on the nose of the aircraft. The pick-offs were potentiometric. The control surface angles were also measured by potentiometers. Continuous trace photographic recorders were used to record the various signals.

3.2.1 Corrections to recorded data

Apart from the free stream total and static pressures, corrected for small pressure errors, the only major parameter requiring correction was sideslip angle β. There are in general, several effects to be considered, but in this case errors arising from boom deflection under inertia and aerodynamic loading can be ignored since the runs were in steady level flight and air loads were relatively low under the conditions flown. Since the analysis relies on changes of sideslip angle, any vane zero offset, due to a calibration datum error or asymmetry arising from manufacturing tolerances, may be neglected.

The position error of a wind vane is the difference between the indicated flow angle and the true free stream direction. It arises from the effect on the local flow of the aircraft and of the boom on which the vane is mounted. The first effect is thought to be negligible in the light of, for example, results from Ref.5. A theoretical calculation of the body influence substantiates this conclusion[6], although the problem has to be greatly simplified to allow analysis.

Tunnel tests on the FD2 nose-boom assembly[7] indicated that for zero sideslip, the incidence vanes, at subsonic speeds, overread by about 8% due to the boom upwash, and this agrees well with simple theoretical calculations[6]. It is thought that as long as the incidence is not high, a correction of 8% to indicated sideslip to allow for the effect of the mounting boom, is also reasonable.

The overall accuracy is estimated at $\pm 0.2^{o}$.

4 TEST TECHNIQUES

The flights were made at an altitude of approximately 40000 ft (12200 m) and Mach numbers ranged from 0.4 to 0.9. The parachute was deployed at the test height at speeds under 250 kn IAS (129 m/s) to avoid the tendency of the pack to come adrift prior to streaming, and to limit the high snatch load which the larger parachute would exert.

Flights were also conducted with the parachute installation fitted, but with the parachute stowed, to establish the basic aircraft trim curves of control deflection *versus* sideslip.

The number of test points which could be achieved in a single flight was limited by the short duration of the aircraft due to its low fuel load, its poor performance with the parachute deployed and also by the relatively high fuel usage during the climb to altitude at the reduced speed associated with pack limitations. The use of reheat to reach the higher Mach number ranges would have aggrevated the fuel problem.

Records were obtained at a number of constant speeds over a range of steady, trimmed sideslips.

The pilots had some difficulty in holding steady conditions under sideslip. Low resolution of the compass and the sensitivity of the artificial horizon presentation to rates and accelerations meant that small rates of yaw may have been present on some runs.

The aileron control circuit was criticised, for aileron stick forces were high and particularly at the larger sideslip angles it was found difficult to achieve small discrete control surface movements due to apparent hysteresis in the system. Use of aileron trim (to back off the stick load) helped considerably although the trimmer circuit was not precise.

Parachute coning undoubtedly increased piloting difficulties and the load fluctuations due to this characteristic may have tended to excite the dutch roll mode. There appears to be no consistent relationship between the onset of coning and indicated airspeed, sideslip angle or parachute size although the coning of the smaller parachute was probably rather more pronounced than that of the larger one, at an included angle of some 10^{o} to 13^{o} (see section 3.1.1). There were some flight conditions, however, in which the parachutes were not coning; at around 230 kn IAS (118 m/s), for example, the smaller parachute was stable. Coning frequencies were generally around 3 Hz and did not appear to vary significantly with indicated airspeed. It would appear that, under most flight conditions, the parachute is entrained in the vortex shed from the wing upper surface[7,8].

In all cases the parachute was successfully released at the conclusion of a test flight and each parachute was used once only.

5 ANALYSIS

5.1 Derivation of rudder power derivative, n_{ζ}

The system of axes used in this analysis is that of wind-body axes.

The parachute yawing moment coefficient is defined by

$$C_{NC} = \frac{N_C}{\frac{1}{2}\rho_0 V_i^2 Sb} \tag{1}$$

where N_C is the parachute yawing moment and the other standard symbols are as defined in the list of symbols.

The full non-dimensional form of the yawing moment equation, including the effect of the parachute, may be written as:

$$i_c\dot{r} - i_e\dot{p} = C_{NC} + n_v\beta + n_r r + n_p p + n_\zeta\zeta + n_\xi\xi \quad . \tag{2}$$

The symbols are defined in the list of symbols.

Under steady conditions equation (2) reduces to

$$C_{NC} + n_v\beta + n_\zeta\zeta + n_\xi\xi = 0 \quad . \tag{3}$$

If the rudder and aileron angles differ by $\Delta\zeta$ and $\Delta\xi$ respectively from the control angles required to trim to the same sideslip angle without the parachute, then by subtraction,

$$\left.\begin{aligned} & n_\zeta\Delta\zeta + n_\xi\Delta\xi + C_{NC} = 0 \\ \text{thus} \quad & n_\zeta = -\frac{(C_{NC} + n_\xi\Delta\xi)}{\Delta\zeta} \quad . \end{aligned}\right\} \tag{4}$$

The increments in rudder and aileron angles may be obtained, respectively, from trim curves of rudder and aileron angle *versus* sideslip, with and without the parachute streamed. Typical such curves are shown in Figs.4 and 5 and it may be seen that the aileron and rudder angles to trim are linear with sideslip angle, and further that the control angle increment is apparently constant over the sideslip range. These characteristics are approximately true for the other trim curves and justify the assumptions of linearity inherent in the analysis. The method of least squares was used to define the best lines through the experimental points. In the present experiment it is found that the aileron contribution in equation (4) is negligible, since n_ξ is thought to be small compared with n_ζ (Ref.9), and $\Delta\xi$ the aileron increment is also small (it is some 0.2°

in the example in Fig.5) and therefore the product $n_\xi \Delta\xi$ is insignificant. N_C was plotted against sideslip, and the intersection at zero sideslip angle was used to derive C_{NC} in the analysis.

5.2 Derivation of the directional stability derivative, n_v

Under conditions of steady sideslip and with the parachute stowed, the yawing moment equation may be written as

$$n_v \beta + n_\xi \xi + n_\zeta \zeta = 0 \qquad (5)$$

and hence

$$n_v = - \left(n_\zeta \frac{d_\zeta}{d_\beta} + n_\xi \frac{d_\xi}{d_\beta} \right) . \qquad (6)$$

The terms d_ζ/d_β and d_ξ/d_β, once the correction to sideslip is applied, become the slopes of the respective trim curves. Although the second term in the bracket is neglected in this analysis since n_ξ is thought insignificant[9], this cannot generally be assumed to be so and a value of n_ξ must then be ascertained from other tests.

5.3 Derivation of C_{NC}, the parachute yawing moment coefficient

With reference to Fig.6, the exact equation for the parachute yawing moment is

$$N_C = P_1 y \cos(\alpha + \theta) + P_2 (x \cos\alpha - z \sin\alpha) \cos\phi + P_3 \left\{ \frac{\sin\phi}{(1 + \tan^2(\alpha + \theta) \cos^2\phi)^{\frac{1}{2}}} (x \cos\alpha - z \sin\alpha) - \frac{\sin(\alpha + \theta) y}{(1 + \tan^2\phi \cos^2(\alpha + \theta))^{\frac{1}{2}}} \right\} \qquad \ldots (7)$$

where P_1 is the parachute load component normal to the post neutral axis in the X-Z plane

P_2 is the parachute load component normal to the post neutral axis in the Y-Z plane

P_3 is the parachute load component parallel to the post neutral axis

x,y,z are the coordinates of the parachute attachment point relative to the aircraft cg

α is the aircraft angle of incidence

θ is the rearwards lean of the post neutral axis relative to the OYZ plane

ϕ is the outwards lead of the post neutral axis relative to the OXZ plane.

The equation is greatly complicated by the inclusion of the terms in ϕ. This angle was only $2^{o}3'$ in the FD2 installation and negligible error is incurred by assuming it zero in the above equation, which then reduces to

$$N_C = P_1 y \cos(\alpha + \theta) + P_2(x \cos\alpha - z \sin\alpha) - P_3 y \sin(\alpha + \theta) \quad . \qquad (8)$$

The first term represents the rearwards load on the post, and is by far the largest one.

P_1 and P_2 were measured directly whereas P_3, the load along the post neutral axis, was obtained from the relationship

$$P_3 = - \left| \left(P_1^2 + P_2^2 \right)^{\frac{1}{2}} \right| \tan\gamma \qquad (9)$$

where γ is the measured cable angle relative to the plane normal to the post neutral axis.

5.4 Effect of rate and inertia terms

The flight records have shown that during most runs, sideslip angle and rates of roll and yaw had oscillatory components at around 0.3 Hz indicating that the dutch roll mode was excited. The effect of the dutch roll on the analysis is negligible if the various damping and inertia terms in equation (2) are negligible compared with the steady state terms. Using existing flight-test extracted derivative values and results obtained from inertia ground tests[10], it was found that the significant terms for typical measured amplitudes of disturbance were the damping-in-yaw $(n_r r)$ and the yaw inertia $i_c \dot{r}$. The amplitude of the former was, at most, a few per cent of the yawing moment due to the parachute (C_{NC}), but the amplitude of the inertia term was as much as 10% of C_{NC} during some runs. Care was taken to analyse only the parts of the records where mean and transient variations were small, but even so some small scatter must be expected.

In addition to displaying the dutch roll tendency of the aircraft, the recorded rates of roll and yaw had a low amplitude signal of about 3 Hz

superimposed and this was thought to be due to the parachute coning behaviour (Fig.7). Since this frequency is an order of magnitude higher than that of the aircraft natural lateral (dutch roll) mode, the aircraft response to a typical amplitude of coning-induced yawing moment oscillation is negligible. Consequently it was thought that the 3 Hz signal recorded was a fuselage bending mode, excited by the coning.

6 RESULTS

6.1 The derivative n_ζ

6.1.1 Results for the rudder power derivative, n_ζ

The results for n_ζ are shown plotted against Mach number in Fig.8. The maximum numerical value is -0.061 at Mach 0.9 and the minimum is -0.053 at Mach 0.55. Also included in the figure are results from Ref.3 where n_ζ is obtained from wind tunnel tests on a 1/9 scale model, and from estimates[11].

6.1.2 Accuracy of the results for n_ζ

Since the increment in aileron angle $\Delta\xi$ in equation (4) was found to be small and the yawing moment due to aileron derivative n_ξ is also thought to be insignificant[9], the aileron contribution in the equation for n_ζ becomes negligible and in this case n_ζ may be derived once C_{NC} and $\Delta\zeta$ are established. The implication arising from $\Delta\xi$ being small is that the sum of the rolling moment exerted by the parachute and that due to the extra rudder angle to trim the parachute load is also small.

Mean values of P_1,P_2 and P_3, the parachute load components, were used in equation (7) to derive N_C, the yawing moment. The post rearwards load had an amplitude of fluctuation generally under some 10% of the mean load, but sometime up to 13%. The maximum instantaneous sideload was generally less than 25% of the mean rearwards load, P_1. The mean sideload was small compared with P_1. The maximum instantaneous load along the post neutral axis was under 15% of P_1 in most cases, and at the higher values for the larger angles of incidence. An example of the behaviour of P_1,P_2 and the cable angle γ is shown in Fig.7.

Since the fluctuations in the loads were not entirely sinusoidal or regular, the mean values cannot be precisely defined and a consequent error of some ±2% in N_C is thought to be incurred. Strain gauge calibration non-repeatability and cross loading effects limited their output to some ±2% uncertainty. Now C_{NC}, the yawing moment coefficient may be obtained from

N_C once the dynamic pressure $\frac{1}{2}\rho V_T^2$ is determined. After the small pressure error corrections have been applied, the dynamic pressure should be reliable to ±1% at the lower speeds (the worst case).

Therefore the root-sum-square error in the individual values of C_{NC} is thought to be some 3%. Since there was apparently no consistent variation in C_{NC} with sideslip angle, the C_{NC} value used for each Mach number band was the mean of the values appropriate to the various points on the trim curves. The standard deviation of C_{NC} at Mach 0.75 is 7%, at Mach 0.8, 4%, and less than 3% for the other conditions.

In order to obtain an insight into the consistency of the parachute drag behaviour, the parachute drag coefficient, C_{DP}, based on the free stream kinetic pressure and the nominal deployed cross-sectional area, was plotted in Fig.9, for both parachute sizes. The variation in C_{DP} for a given parachute is some ±5% except for one particular parachute when the scatter is about ±8%. The overall bandwidth for all except one of the parachutes is some ±10% (neglecting a dubious point) and this is encouraging since a parachute's streamed area, and therefore drag characteristic, is likely to vary from sample to sample.

However, C_{DP} values for one parachute are a fairly consistent 12% higher than the mean of the other parachutes. This is thought to be genuine since the rudder angle increments to trim also appear large.

The measured drag coefficients of both sizes of parachute are greater than unity, which is the manufacturer's quoted value. However, this is not unexpected since the parachute is in the vicinity of the wing vortex and local flow velocities are probably higher than the free stream.

Rudder angles may be determined to some $\pm 0.2^{\circ}$, but the accuracy of $\Delta\zeta$ is degraded further by the poor definition of some of the curves through the trim points for ζ *versus* β. This is mainly a consequence of the small number of points on the trim curves, and the error in $\Delta\zeta$ may be as high as ±7% for some Mach numbers.

It is thought, then, that the root-sum-square error in n_ζ is some 10% at Mach 0.75 and about 8% at the other Mach numbers. The majority of the parachute-deployed points on the Mach 0.75 and 0.8 trim curves (where the results for n_ζ appear low) are from one flight and the values of C_{NC} are consistently lower than the few from the other flights appropriate to these conditions. It may be that an undetermined experimental error is responsible but the results must be accepted in the absence of any explanation.

6.1.3 Comparison of n_ζ with wind tunnel values

The wingtip parachute flight tests reveal that n_ζ is considerably lower in magnitude than wind tunnel results suggest. The latter value for n_ζ is approximately -0.095 whereas the flight results range between -0.053 and -0.061. Estimates for n_ζ (Ref.11) values are smaller than those from the tunnel tests but must be considered approximate anyway since, for example, no allowance was made for the brake parachute fairing at the base of the fin and rudder which results in a large gap between rudder and fuselage when the former is deflected.

One possible reason for the much higher tunnel values of n_ζ is the unrepresentative nature of the model in that the tunnel sting assembly was attached to the rear fuselage and the reheat nozzle was omitted. The model tests were made with the intake flow represented but the efflux was from an annular gap around the sting which is markedly different from the jet efflux from the aircraft. The mass flow and momentum were also not representative. However, this rear end distortion is unlikely to have a substantial effect on n_ζ.

The model was tested at the trimmed incidence appropriate to the test Mach number at 40000ft (12200m) altitude, but not at the appropriate elevator trim angles. Two model elevator settings were used, namely 4.8° and 9.8° up and the results for the former condition are plotted in Fig.8. The values appropriate to 9.8° up elevator are only some 10% lower than for the other condition, which itself is approximately the mean of the flight elevator settings, so apparently the effect of elevator deflection on n_ζ does not help to account for the discrepancy.

The second possibility is that the flow fields round the model and aircraft fins are significantly different. Since the Reynolds numbers involved in the tunnel tests are much lower than flight values, it is to be expected that the scale rate of boundary layer growth is greater on the model and this may result in a modified flow pattern round the rear fuselage.

It is felt, however, that the main reason for the discrepancy is aeroelastic distortion. When the fin is subject to sideslip, it will twist so as to reduce the loading, and a deflected rudder might be expected to significantly increase this effect, depending on the sense of deflection. The rudder itself may suffer deformation and the nett result would be a significant lowering of n_ζ.

The effect would be expected to be less marked at the lower Mach numbers where dynamic pressure is low and it is surprising that the flight results show

no sign of a recovery in n_ζ with decreasing speed. It may be that a deterioration in the derivative with increasing incidence is suppressing any such recovery.

6.2 The derivative n_v

6.2.1 Results for the directional stability derivative n_v

The results for n_v are shown plotted against Mach number in Fig.10, which includes those from wind tunnel tests on the 1/9 scale model[2,3] and from flight tests. The latter involved dutch roll manoeuvres subsequently analysed by the time vector method[4]. These n_v values are re-analysed from Ref.4 to incorporate the measured moments of inertia[10]. The minimum value of n_v from the wingtip parachute tests is 0.058 at Mach 0.75 and the maximum is 0.077 at Mach 0.9. The trough at Mach 0.75 and 0.8 would appear to be a reflection of the n_ζ characteristic at these Mach numbers.

6.2.2 Accuracy of the results for n_v

It has been shown that the derivative n_v is obtained from the expression $n_v = -\left(n_\zeta \frac{d_\zeta}{d_\beta} + n_\xi \frac{d_\xi}{d_\beta}\right)$. The possible root-sum-square error in n_ζ has been shown to be about 8 to 10%, and the error in d_ζ/d_β is some ±4% for Mach numbers up to 0.7, and less, around ±3% for the higher Mach numbers.

Since the aileron contribution $(n_\xi(d_\xi/d_\beta))$ to n_v is thought negligible, the root-sum-square error in n_v is about 11%.

6.2.3 Comparison of n_v with other results

The values of n_v extracted by the technique described in this paper are in reasonable agreement with those from the flight tests of Ref.4 but there is an insufficient number of experimental points to justify drawing a mean line in either case.

The wind tunnel tests produced values higher than the flight tests, the discrepancy being some 15% to 20% (Fig.10). The shapes of the respective variations with Mach number given by the tunnel tests and the present results are not inconsistent within the scatter on the flight results. The results from the dutch roll flight analysis, however, suggest less variation with Mach number.

6.2.4 Discussion of n_v

The agreement in n_v between the two flight test techniques is within the accuracy expected from the present results (although the apparent insensitivity

of the Ref.4 results to Mach number is surprising) and this is encouraging since the implication is that a representative value of n_ζ has been used in the present analysis.

It has already been mentioned that the absence of a representative jet efflux from the tunnel model might have an effect on n_ζ, and this may also be true for n_v. It is known that the efflux can have a substantial effect on n_v at supersonic speeds[12], although it is probably not nearly so apparent under subsonic conditions.

The flight trials of Ref.4 were conducted with the rudder nominally undeflected and so the effects of rudder-induced aeroelasticity on n_v would be absent. However, since in the present analysis, n_v has been derived from trim curves of rudder angle *versus* sideslip, the derivative must be affected to some extent. It is not possible to state whether this might result in a significant difference between the values for n_v extracted from the two flight techniques. Certainly a difference between flight and tunnel test values of n_v is to be expected since, in sideslipped flight there will be fin distortion even for zero rudder deflection, whereas the model is relatively extremely rigid.

Finally, it has been mentioned that the derivative n_ξ is assumed negligible under the conditions described in Ref.8 which are fairly similar to those for the wingtip parachute tests. It is possible that n_ξ is dependent on sideslip, and this may therefore affect the trim curve slope d_ζ/d_β since aileron angle to trim will vary with sideslip angle. Any such effect would be apparent on the wingtip parachute results alone.

7 CONCLUSIONS

The wingtip parachute technique yielded values of the derivative n_ζ to a root-sum-square accuracy of 10% and the derivative n_v to some 11%.

The technique was found satisfactory except for a coning problem where the parachute was believed to be entrained in the wing vortex. The effect was not marked enough to jeopardise the analysis, though it introduced further scatter on the results and could be very significant in the case of the slender delta configuration with its attendant strong vortex wake. The only way of ensuring that the parachute streams clear of the wake appears to be by attaching it to the tip of a lateral post emanating from the wingtip (as in later tests, on the HP 115 research aircraft[13]).

The technique can be expensive in terms of the number of flights required to define the derivative over a range of conditions, particularly for aircraft where limited fuel capacity can severely curtail the number of runs available per flight.

Encouragingly, n_v is in reasonable agreement with other flight tests.

The results indicate that the wind tunnel tests yielded values of n_ζ and n_v which were too large. Aeroelasticity is thought to be the main reason for the discrepancy but the necessary geometric distortion of the model, the effects of the unrepresentative jet efflux and of Reynolds number may be contributory. The derivative n_ξ is believed to be insignificant in the analysis of the present tests but this is not true in the general case and, therefore, n_v cannot always be derived from a knowledge of n_ζ and the rudder angle *versus* sideslip trim curves alone.

Table 1

FAIREY DELTA 2 - PRINCIPAL DIMENSIONS

Wing	
Gross area	33.45 m^2
Span	8.18 m
Centre-line chord	7.62 m
Tip chord	0.56 m
Mean aerodynamic chord	5.11 m
Leading-edge sweep	59.9°
Dihedral	0°
Twist	0°
Wing-body angle	$+1.5^\circ$
Fin and rudder	
Fin plus rudder area	3.48 m^2
Rudder area	0.85 m^2
Fin leading-edge sweep	60.7°
Rudder hinge-line sweep	42.5°
All-up-weights at take off	61900 N
Centre of gravity position (mid-fuel)	31.5% mean aerodynamic chord

SYMBOLS

b	aircraft span, m
C_{DP}	parachute drag coefficient, $C_{DP} = \dfrac{D_P}{\frac{1}{2}\rho_0 V_i^2 S}$
C_{NC}	parachute yawing moment coefficient, $C_{NC} = \dfrac{N_C}{\frac{1}{2}\rho_0 V_i^2 Sb}$
D_P	parachute drag, N
I_C, i_C	dimensional and non-dimensional yaw inertia
I_E, i_E	dimensional and non-dimensional product of inertia
M	Mach number
N_C	parachute yawing moment (+ve for nose to starboard), N m
n_p	yawing moment derivative due to rate of roll, rad^{-1}
n_r	yawing moment derivative due to rate of yaw, rad^{-1}
n_v	yawing moment derivative due to sideslip, rad^{-1}
n_ζ	yawing moment derivative due to rudder, rad^{-1}
n_ξ	yawing moment derivative due to aileron, rad^{-1}
OX,OY,OZ	body datum axes. O is at the centre of gravity
P_1	parachute load component normal to the post neutral axis in the OX-OZ plane (+ve forwards), N
P_2	parachute load component normal to the post neutral axis in the OY-OZ plane (+ve to starboard), N
P_3	parachute load component parallel to the post neutral axis (+ve downwards), N
p	rate of roll, rad/s or deg/s
$\dot{p}$	angular acceleration in roll, rad/s^2 or deg/s^2
r	rate of yaw, rad/s or deg/s
$\dot{r}$	angular acceleration in yaw, rad/s^2 or deg/s^2
S	aircraft wing area, m^2
V_i, V_T	equivalent airspeed and true airspeed, kn or m/s
x,y,z	coordinates of parachute attachment point relative to the aircraft centre of gravity, m
α	aircraft incidence, degrees
β, β_i	aircraft true sideslip angle and indicated sideslip angle, degrees or rad
γ	angle between parachute cable and the plane normal to the post neutral axis, (+ve downwards), degrees
$\zeta, \Delta\zeta$	rudder angle and increment in rudder angle (in plane parallel to aircraft centre line), degrees or rad

SYMBOLS (concluded)

θ	rearwards lean of the post neutral axis relative to the OYZ plane, +ve rearwards, degrees
$\xi, \Delta\xi$	aileron angle and increment in aileron angle (relative to hinge-line) degrees or rad
ρ, ρ_0	ambient and sea level air density, kg/m^3
ϕ	outwards lean of the post neutral axis relative to the OXZ plane, (+ve outwards), degrees

REFERENCES

No.	Author	Title, etc.
1	F.W. Dee	Proving tests of a wingtip parachute installation on a Venom aircraft, with some measurements of directional stability and rudder power. ARC CP 658 (1962)
2	T.A. Cook R.W. Hayward	Force measurements on a 1/9 scale model of the FD2 research aircraft at Mach numbers between 0.6 and 1.8. RAE Technical Report 68294 (ARC 31236) (1968)
3	D. Morton	Force and moment tests on a 1/9th scale model Fairey delta 2 aircraft. ARA Model Test Notes M6/1 and 2 (1964)
4	R. Rose	Flight measurements of the dutch roll characteristics of a 60 degree delta wing aircraft (Fairey Delta 2) at Mach numbers from 0.4 to 1.5 with stability derivatives extracted by vector analysis. ARC CP 653 (1961)
5	N.M. McFadden G.R. Holden J.W. Ratcliffe	Instrumentation and calibration technique for flight calibration of angle-of-attack systems on aircraft. NACA TIB 3522
6	Danforth Letko	Theoretical investigation at subsonic speeds of the flow ahead of a slender inclined parabolic-arc body of revolution, and correlation with experimental data obtained at low speeds. NACA TN 3205 (1954)
7	F.W. Dee D.G. Mabey	Wind tunnel calibration of incidence vanes for use on the Fairey ER 103. RAE Technical Note Aero 2785 (1961)
8	F.W. Dee O.P. Nicholas	Flight determination of wing flow patterns and buffet boundaries for the Fairey Delta 2 aircraft at Mach numbers between 0.4 and 1.3, and comparison with wind tunnel results. ARC R&M 3482 (1964)

REFERENCES (concluded)

No.	Author	Title, etc.
9	F.W. Dee	Flight measurements at subsonic speeds of the aileron rolling power and lateral stability derivatives ℓ_v and y_v on a 60^o delta wing aircraft (Fairey Delta 2). ARC CP 739 (1963)
10	C.S. Barnes A.A. Woodfield	Measurement of the moments and product of inertia of the Fairey Delta 2 aircraft. ARC R&M 3620 (1968)
11		Royal Aeronautical Society Data Sheets - Aerodynamics. (5 volumes)
12	C.H. Wolowicz E.C. Hollerman	Stability - derivative determination from flight data. AGARD Report 224 (1958)
13	R.L. Poulter	Measurement of the yawing moment of inertia of an aircraft (HP115) in flight. ARC R&M 3691 (1970)

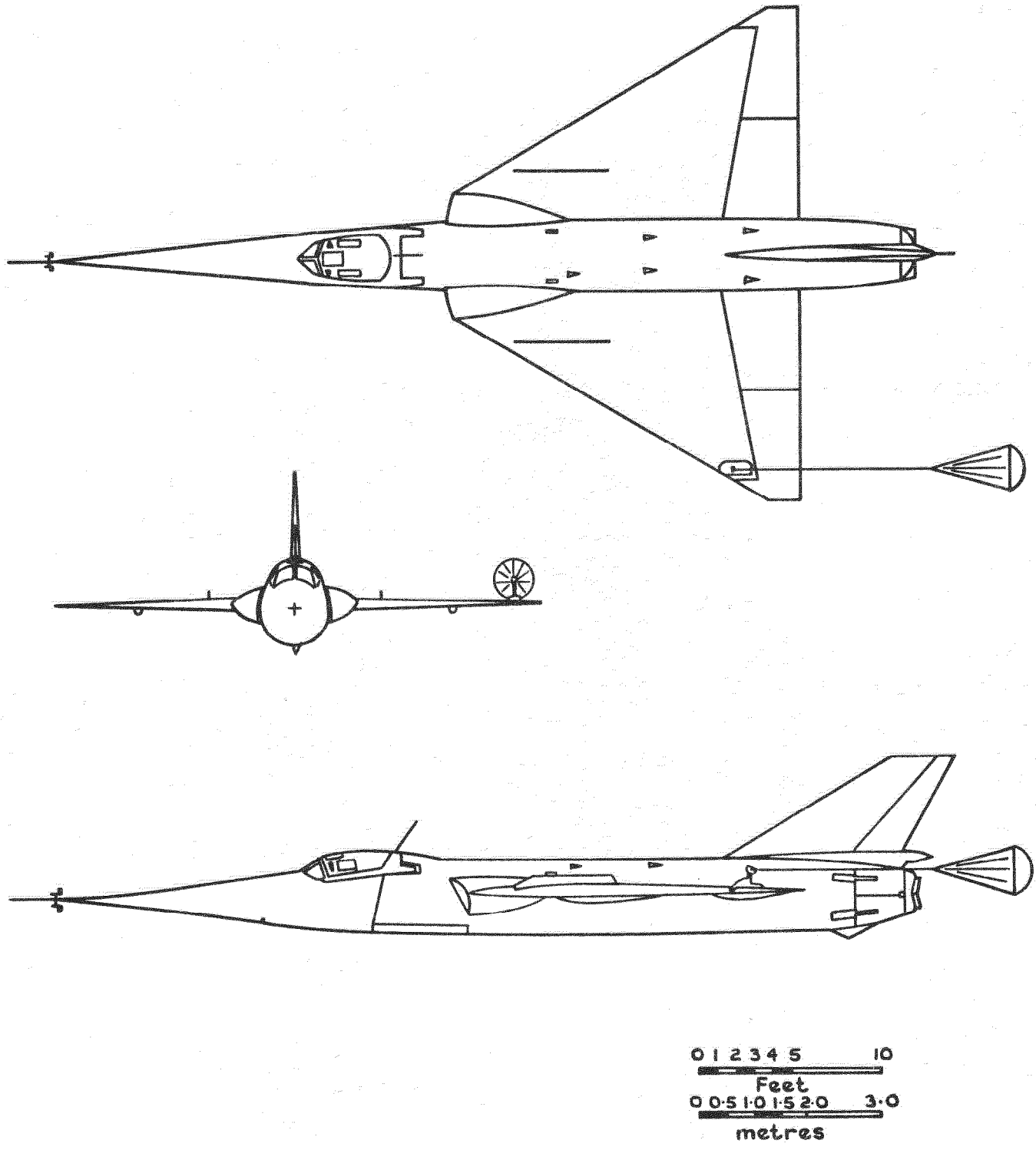

Fig. 1 G A of Fairy Delta 2 with 30" (0·76 m) dia parachute deployed

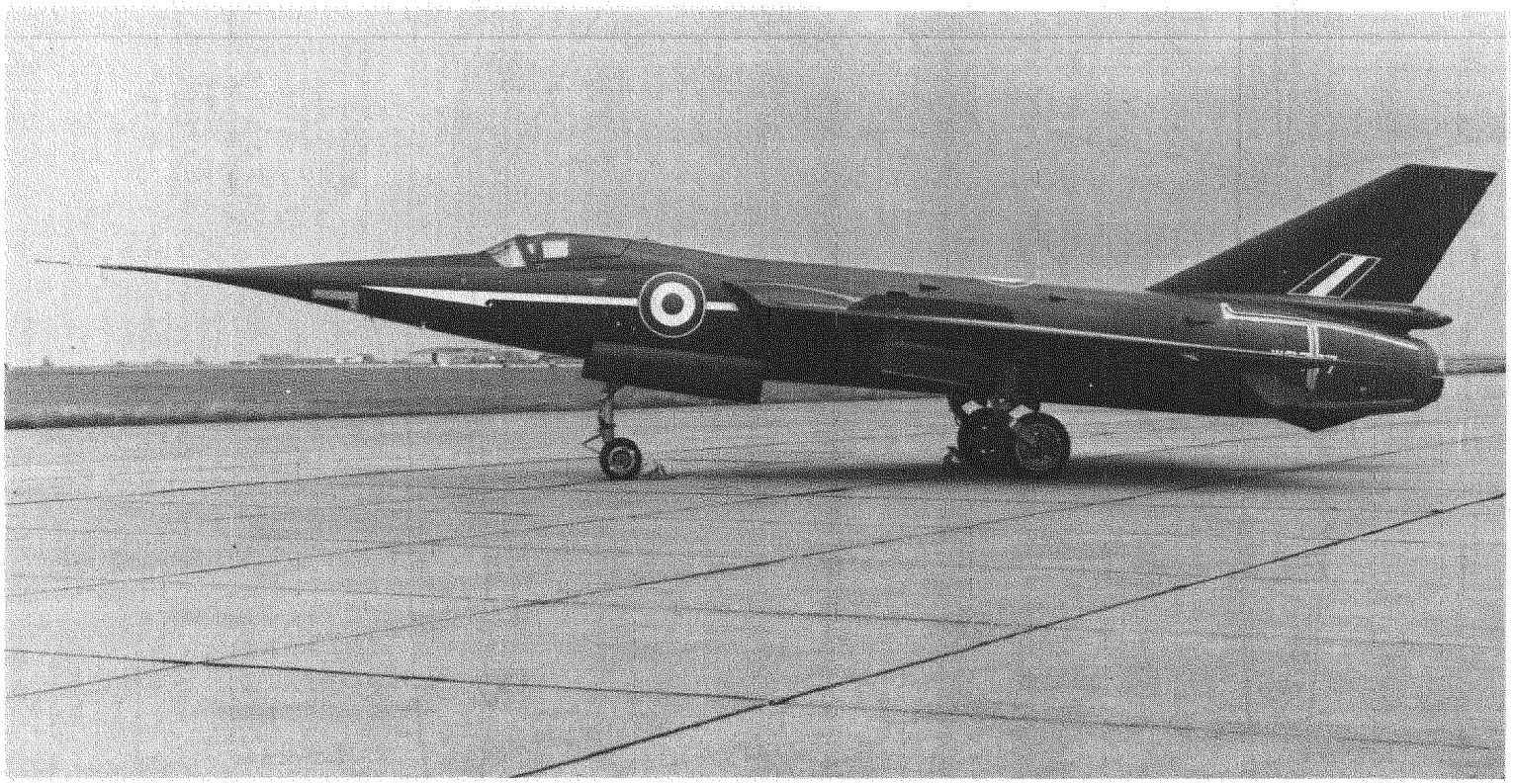

Fig.2 The Fairy Delta 2 research aircraft

Fig.3 Parachute post installation on port wing-tip

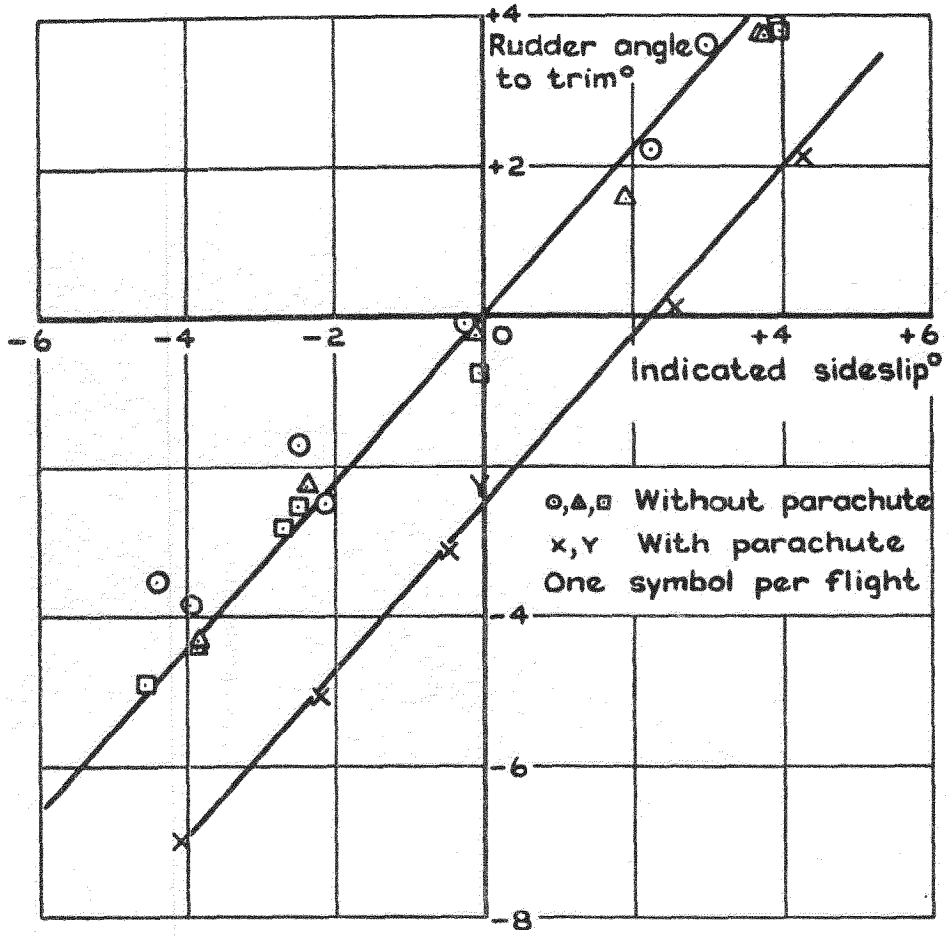

Fig.4 Typical rudder angle – sideslip trim curves, with and without the 18in (0·46m) dia parachute
0·73 → 0·77M

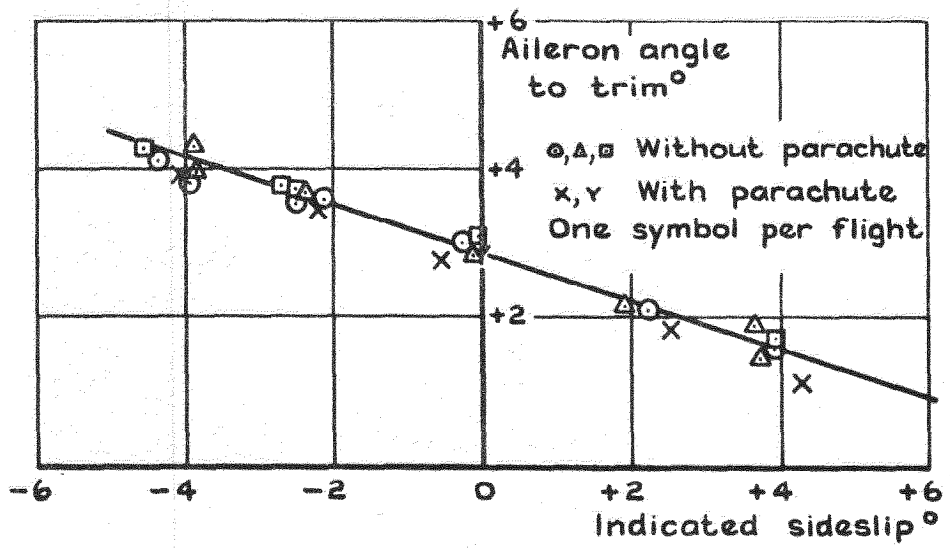

Fig. 5 Typical aileron angle – sideslip trim curves, with and without the 18in (0·46m) dia parachute
0·73 → 0·77M

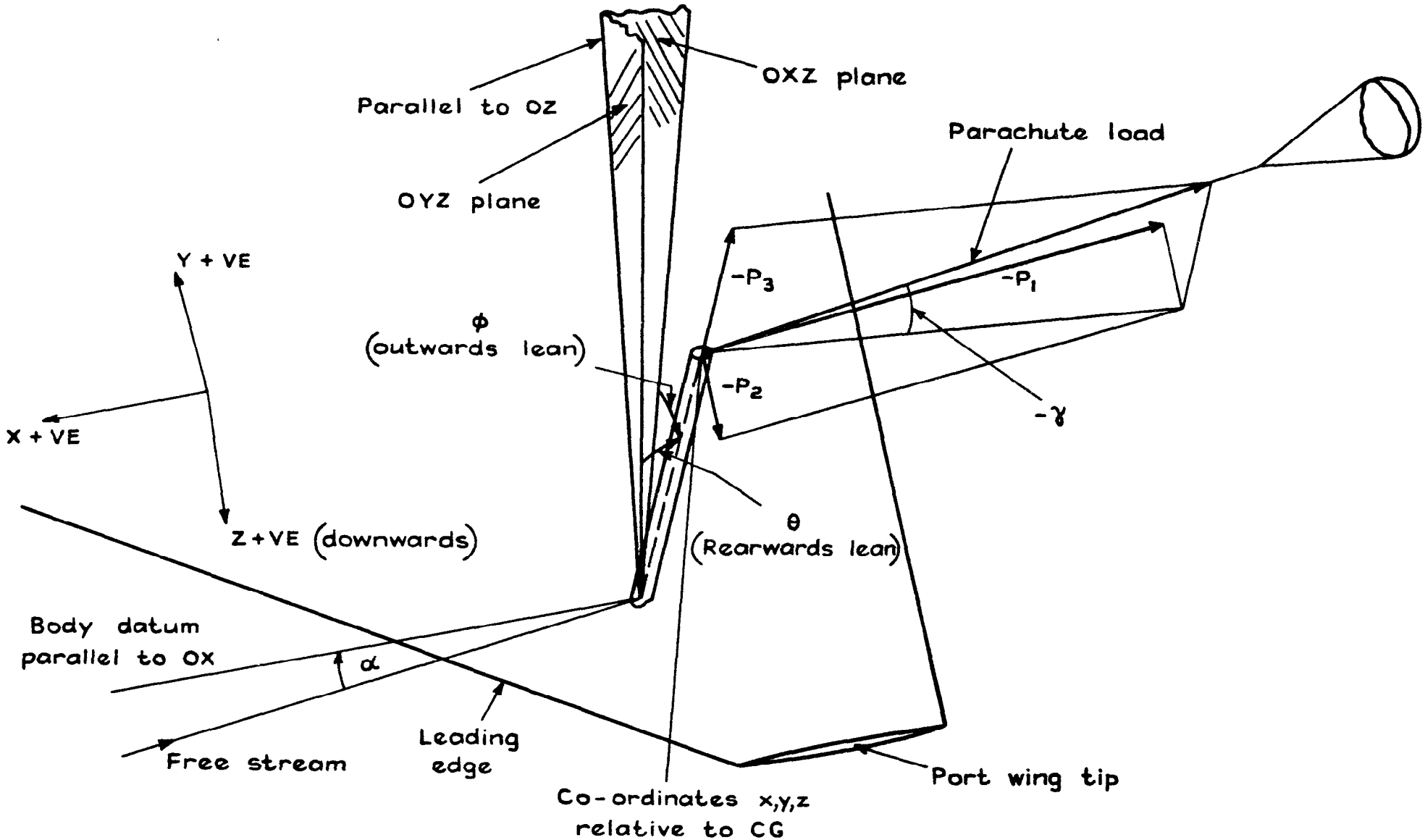

Fig. 6 Illustration for the derivation of parachute yawing moment

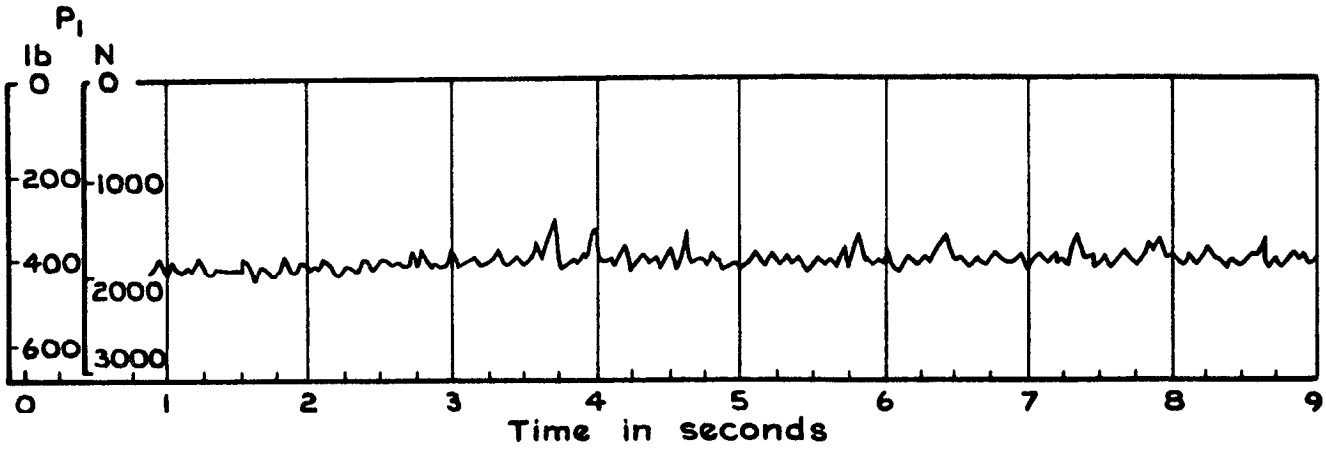

a Parachute rearwards load, P_1

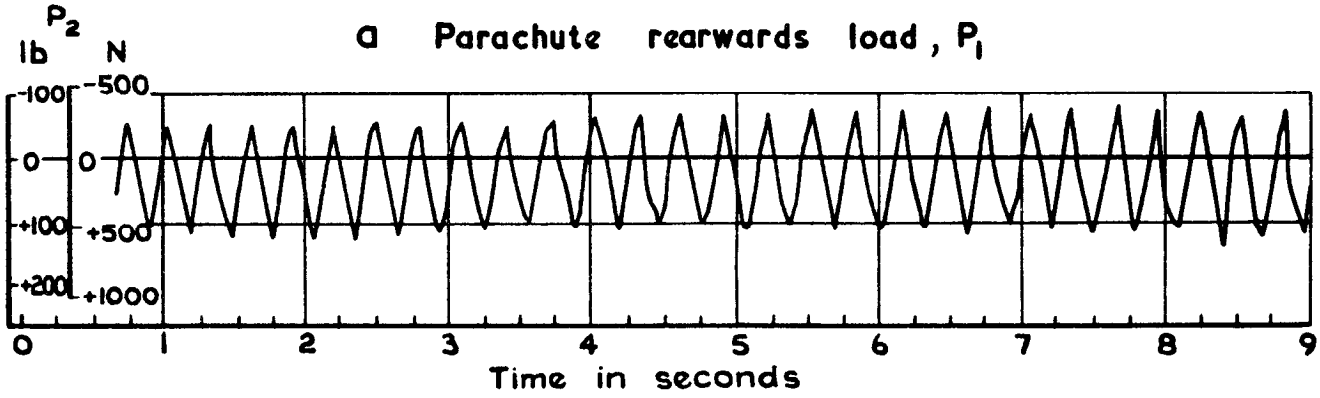

b Parachute sideload, P_2

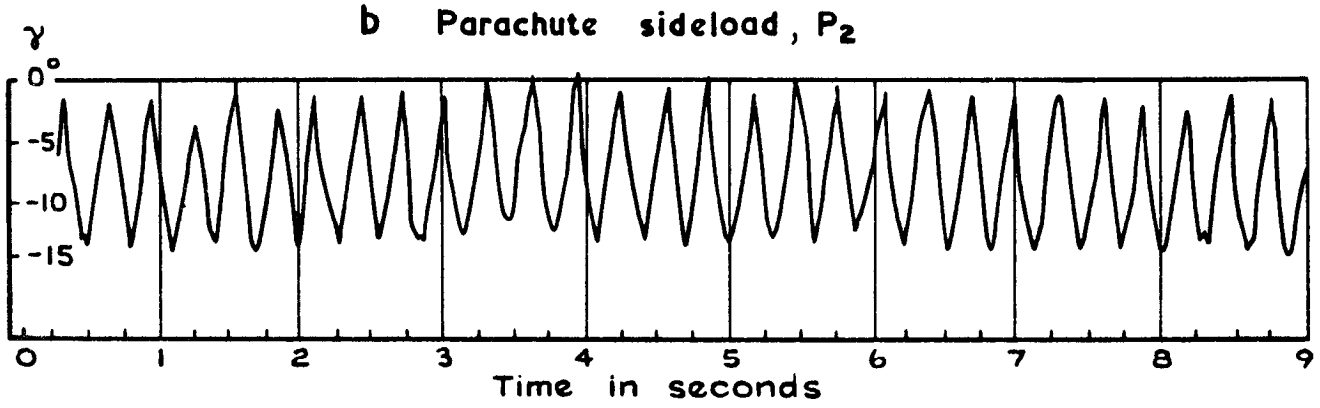

c Parachute cable angle, γ

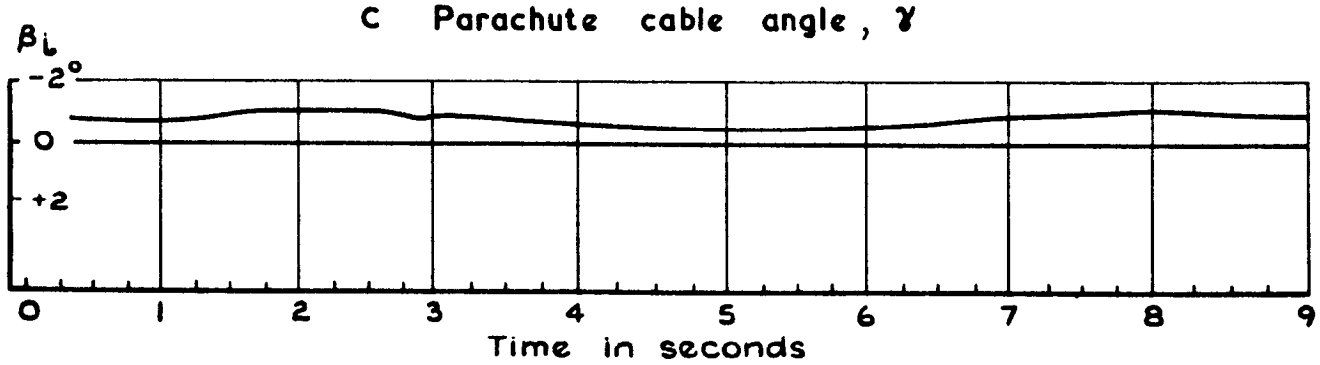

d Indicated sideslip angle, β_i

Fig.7 Typical flight record with 30in (0·76m) diameter parachute deployed. V_i = 178 kn at 39000 ft (11885 m) altitude

Current Paper 1298

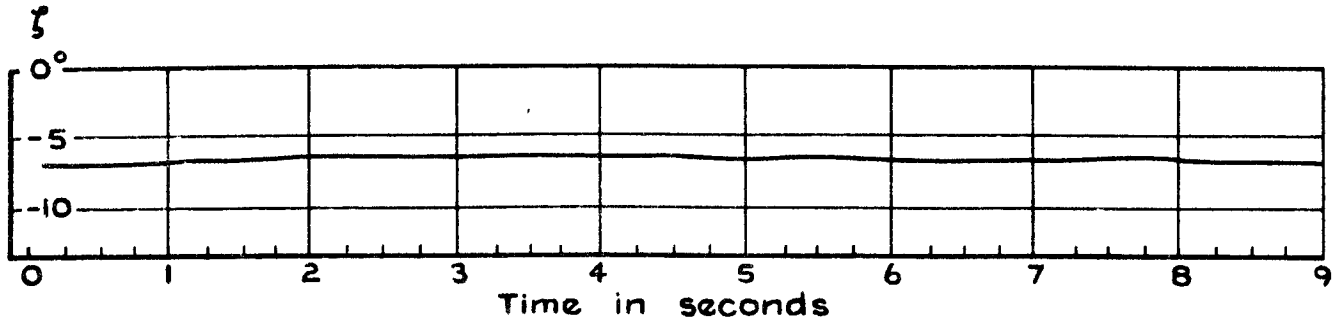

e Rudder angle, ζ

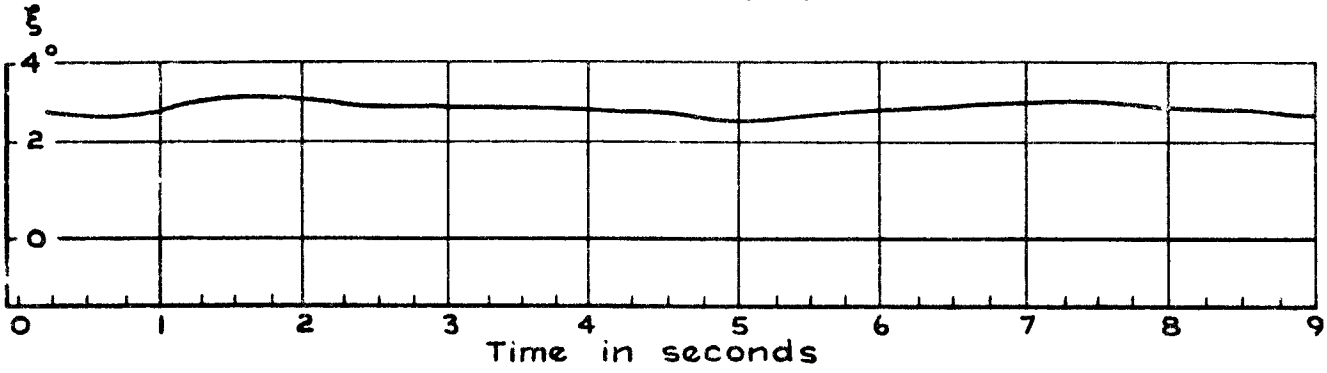

f Port aileron angle ξ, (relative to wing chord)

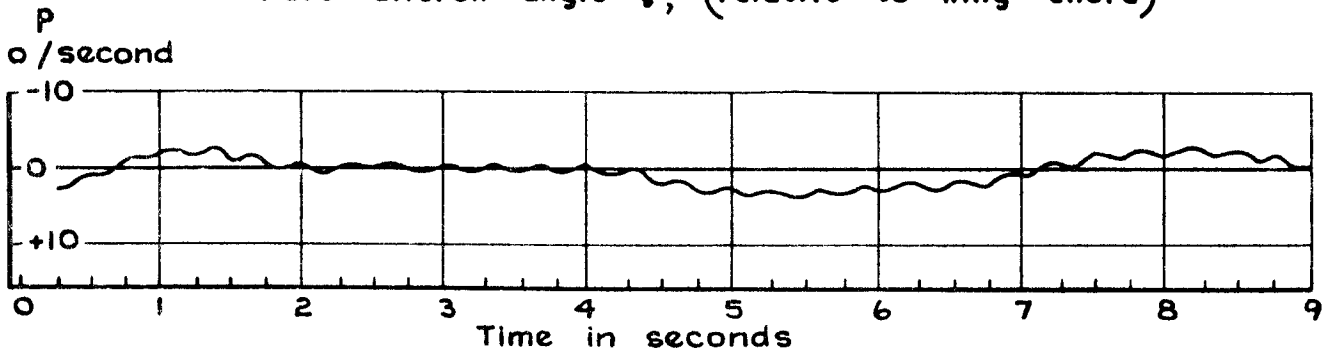

g Rate of roll, p

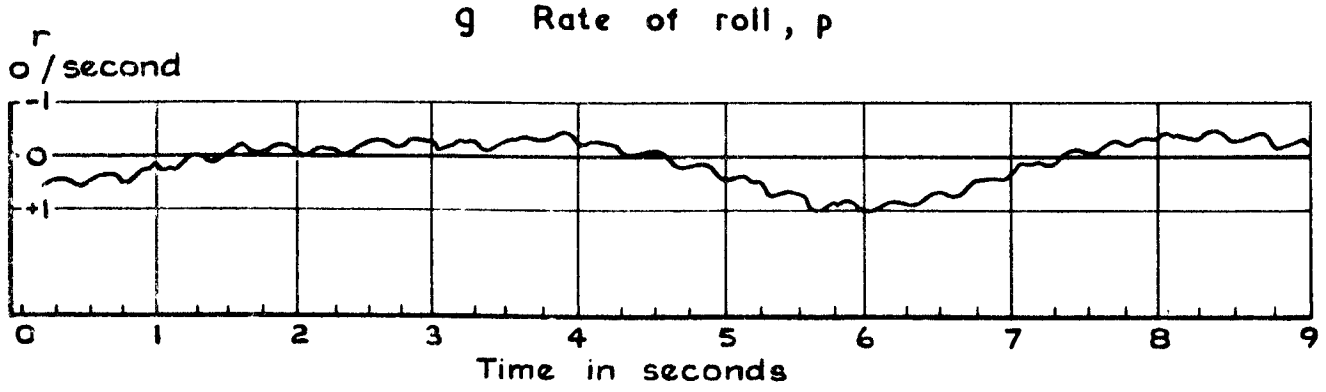

h Rate of yaw, r

Fig.7 contd Typical flight record with 30in (0·76m) diameter parachute deployed. V_i = 178kn at 39000ft (11885m) altitude

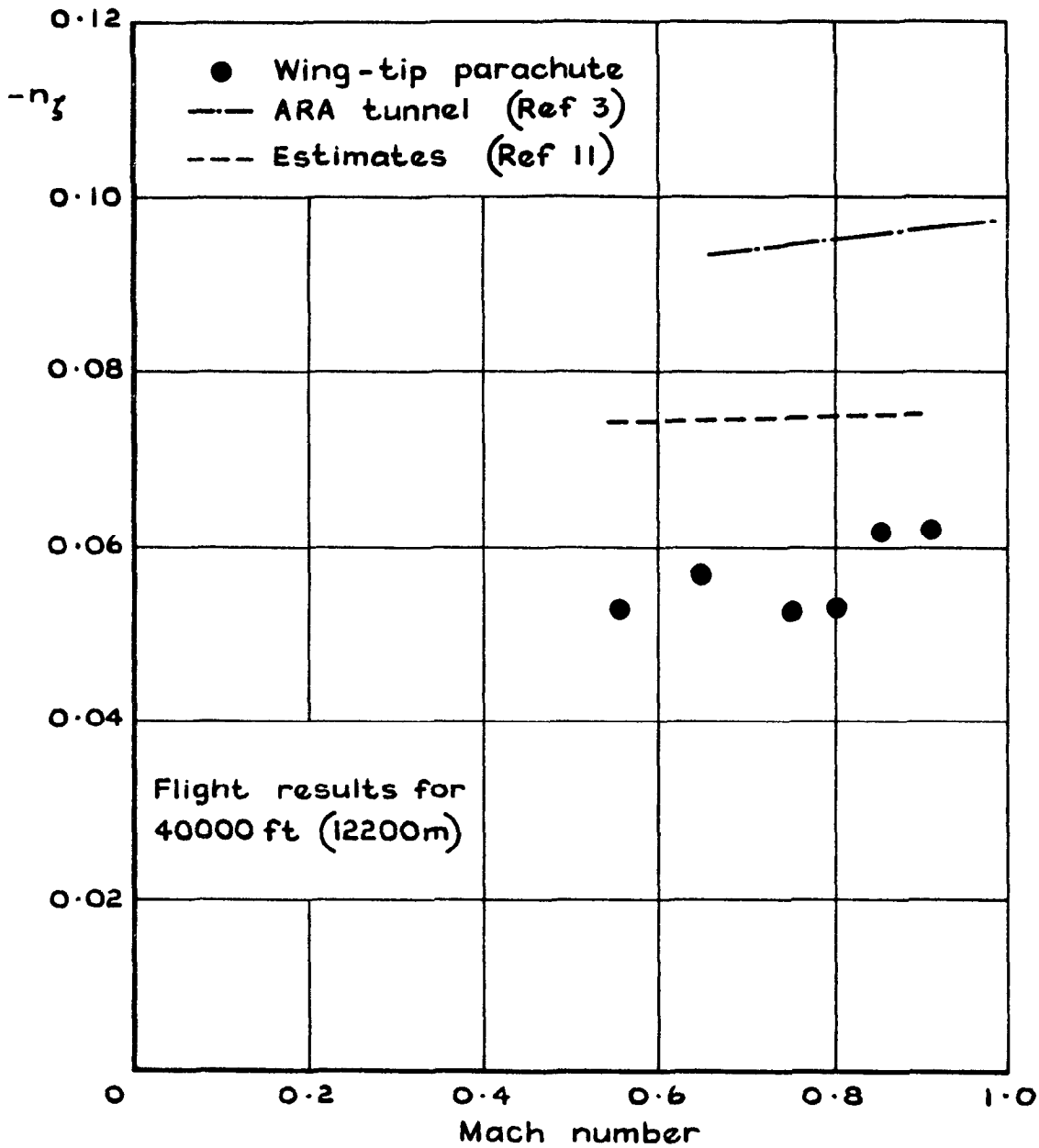

Fig. 8 Rudder power derivative, n_ζ, against Mach number, and comparison with other results

Current Paper 1298

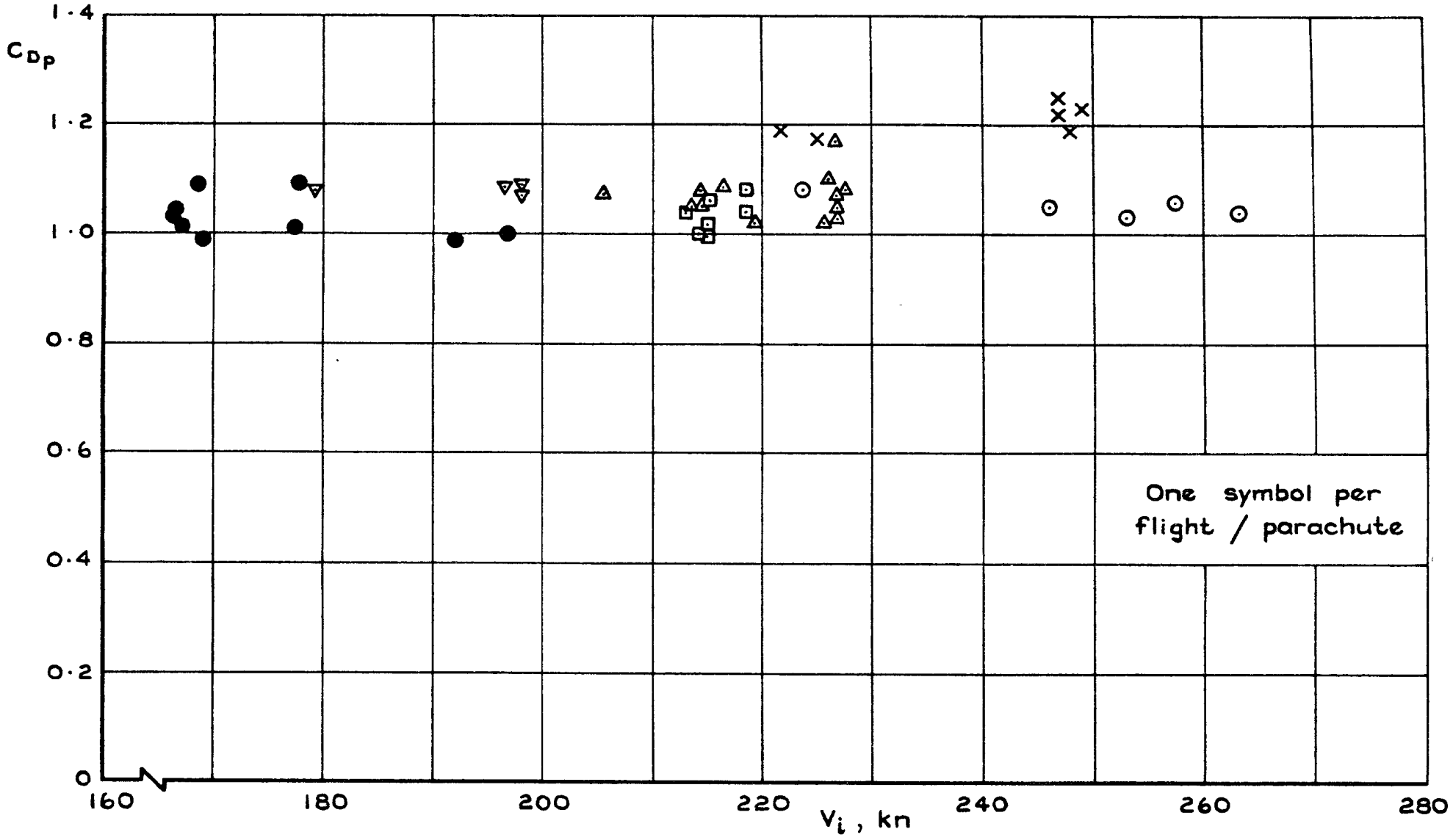

Fig. 9 Parachute drag coefficient, C_{D_P}, against equivalent airspeed, V_i

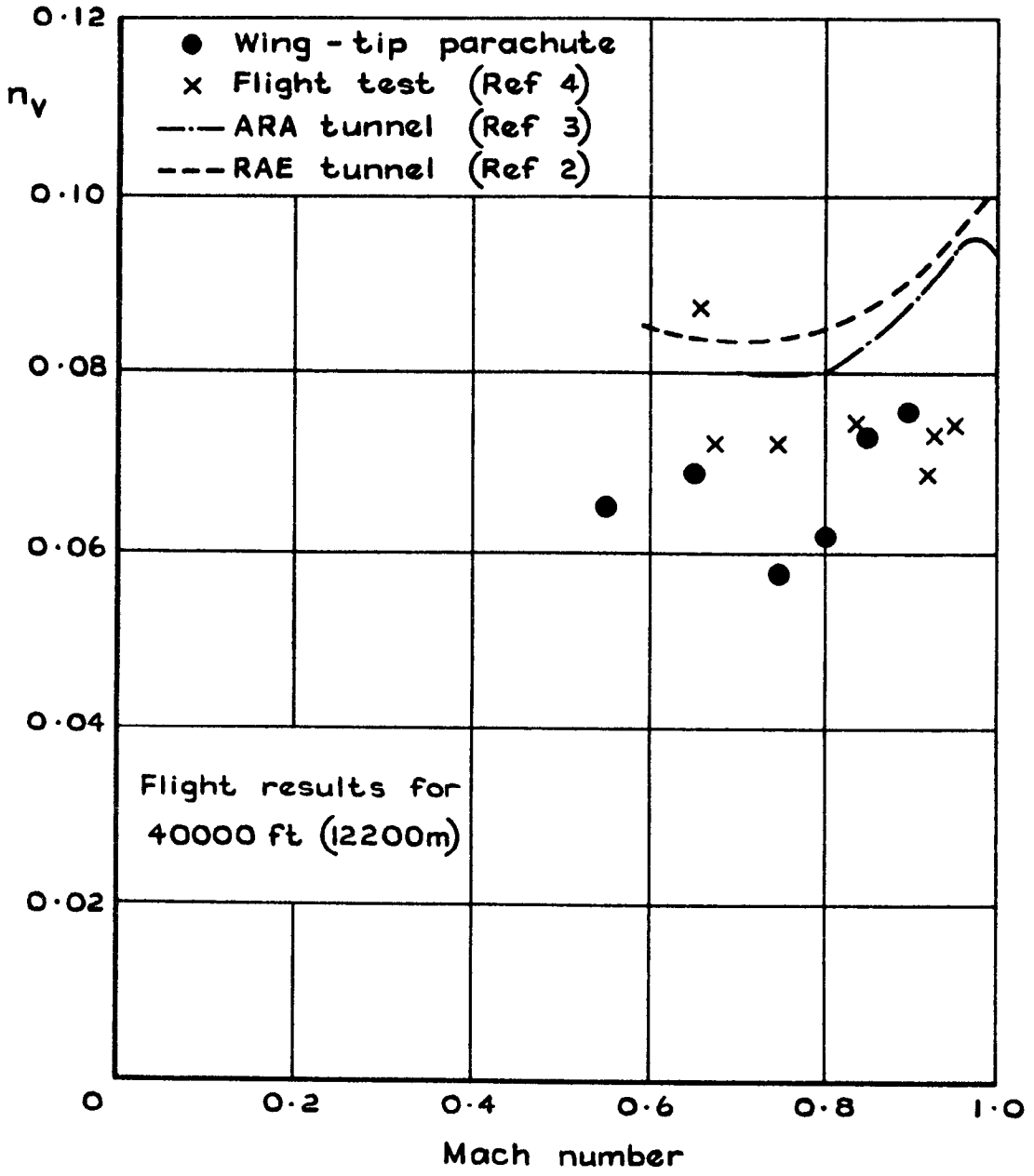

Fig. 10 Directional stability derivative, n_v, against Mach number, and comparison with other results

Printed in England for Her Majesty's Stationery Office by the Royal Aircraft Establishment, Farnborough. Dd. 505376 K4 7/74.

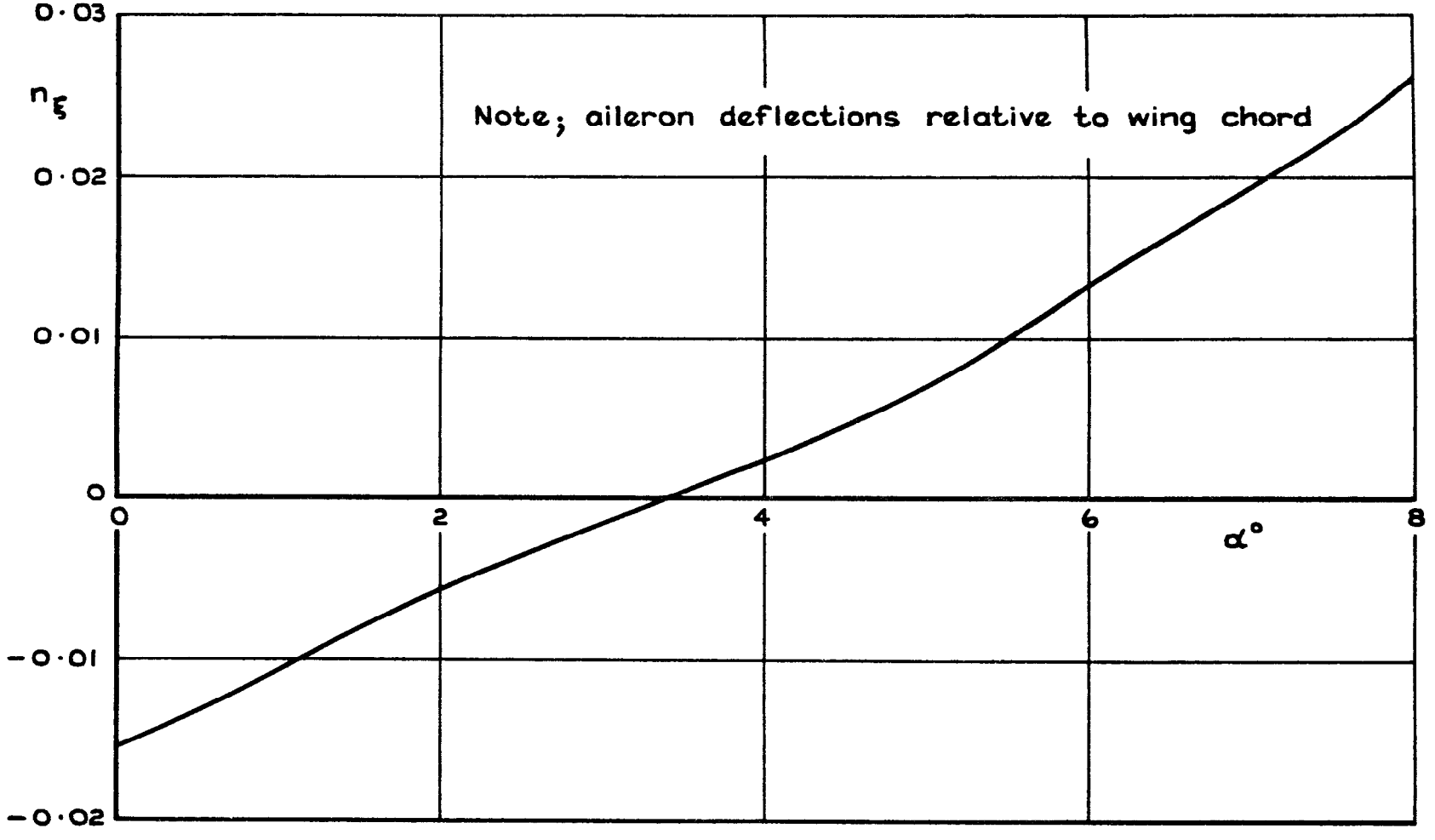

Fig. 11 Yawing moment due to aileron deflection derivative, n_ξ, obtained from tunnel tests of Ref 4

ARC CP No.1298
February 1973

533.694.542 :
533.6.013.415 :
533.666.2

Ingle, G.

FLIGHT DETERMINATION OF THE RUDDER POWER AND DIRECTIONAL STABILITY OF THE FAIREY DELTA 2 AIRCRAFT USING A WINGTIP PARACHUTE

The wingtip parachute technique has been used to extract the rudder power derivative, n_ζ, for the Fairey Delta 2 research aircraft. The flight tests have revealed that n_ζ has a considerably smaller value than tunnel tests suggested, and it is believed that this is due to the aeroelasticity of the fin and rudder, and possibly to unrepresentative flow over the rear of the wind-tunnel model.

Once n_ζ was obtained, the directional stability derivative, n_v, was derived on the assumption that the derivative n_ξ was small. The values of the derivative n_v obtained by this technique agree well with those from other flight tests and reasonably well with tunnel test results.

Cut here

ARC CP No.1298
February 1973

533.694.542 :
533.6.013.415 :
533.666.2

Ingle, G.

FLIGHT DETERMINATION OF THE RUDDER POWER AND DIRECTIONAL STABILITY OF THE FAIREY DELTA 2 AIRCRAFT USING A WINGTIP PARACHUTE

The wingtip parachute technique has been used to extract the rudder power derivative, n_ζ, for the Fairey Delta 2 research aircraft. The flight tests have revealed that n_ζ has a considerably smaller value than tunnel tests suggested, and it is believed that this is due to the aeroelasticity of the fin and rudder, and possibly to unrepresentative flow over the rear of the wind-tunnel model.

Once n_ζ was obtained, the directional stability derivative, n_v, was derived on the assumption that the derivative n_ξ was small. The values of the derivative n_v obtained by this technique agree well with those from other flight tests and reasonably well with tunnel test results.

Cut here

DETACHABLE ABSTRACT CARDS

DETACHABLE ABSTRACT CARDS

Published by
HER MAJESTY'S STATIONERY OFFICE

To be purchased from
49 High Holborn, London WC1V 6HB
13a Castle Street, Edinburgh EH2 3AR
41 The Hayes, Cardiff CF1 1JW
Brazennose Street, Manchester M60 8AS
Southey House, Wine Street, Bristol BS1 2BQ
258 Broad Street, Birmingham B1 2HE
80 Chichester Street, Belfast BT1 4JY
or through booksellers

C.P. No. 1298

ISBN 011 470882 7